and hence a reduced flow rate in the pressure-drop direction. This reduced flow rate seems to suggest that the liquid have an apparent higher viscosity. The apparent viscosity is called the electro-viscosity.

Cross References

► Streaming Current and Electroviscosity

Electrowetting

Leslie Yeo[1], Hsueh-Chia Chang[2]
[1] Micro/Nanophysics Research Laboratory Department of Mechanical Engineering, Monash University, Clayton, VIC, Australia
[2] Center for Microfluidics and Medical Diagnostics Department of Chemical & Biomolecular Engineering, University of Notre Dame, Notre Dame, IN, USA
leslie.yeo@eng.monash.edu.au

Synonyms

Electrocapillary effect; Electrowetting on dielectric (EWOD); Electrowetting on insulator coated electrodes (EICE); Electrowetting on line electrodes (ELE)

Definition

Electrowetting concerns the use of an externally applied electric field to actuate or manipulate small volumes of liquid by altering its interfacial tension and hence the macroscopic contact angle or by inducing bulk liquid motion through an interfacial electric stress.

Chemical and Physical Principles

Electrowetting derives its roots from early observations of electrocapillary phenomena by Gabriel Lippmann in 1875, who noted variations in interfacial tension as an electric potential is applied between an electrolyte solution in direct contact with a metal, in this case, mercury. This culminated in the classical Lippmann equation:

$$\left.\frac{\partial \gamma}{\partial V}\right|_{T,p,\mu} = -\frac{CV}{A}\,, \tag{1}$$

where γ is the interfacial tension (between the metal and electrolyte), V the applied potential, T the temperature, p the pressure and μ the chemical potential. The right hand side of Eq. (1) is the surface charge density, where C is the capacitance with cross sectional area A and separation d. Since $C = \varepsilon_0\varepsilon_1 A/d$, where ε_0 is the permittivity of free space and ε_1 the liquid dielectric constant, Eq. (1) can be written as

$$\Delta\gamma = -\frac{\varepsilon_0\varepsilon_1}{2d}V^2\,. \tag{2}$$

The term on the right hand side of Eq. (2) is hence the electrocapillary force per unit length (linear force density) in the solid plane along the contact line.

Strictly, the term *electrocapillarity* therefore refers to the change in the solid or liquid metal–electrolyte interfacial tension, as shown in Fig. 1a. For the principle to be practical, however, it was necessary to avoid electrolysis of the aqueous solution. This was later overcome by coating the electrode surface with a thin dielectric layer (e. g., polymer substrate) several microns to millimeters in thickness, from which the term *electrowetting-on-dielectric* (EWOD) or *electrowetting on insulator coated electrodes* (EICE) arises [1], as shown in Figs. 1b and 1c. In cases where the insulating layer is not hydrophobic (e. g., parylene), a very thin hydrophobic layer such as a fluoropolymer of order nanometers in thickness, is coated onto the insulator.

In general, the term *electrowetting*, at least for EWOD or EICE configurations in which spontaneous spreading does not occur and hence the contact angles are *static* (we shall deal with the case of *spontaneous electrowetting* below), has traditionally been associated with the change in the macroscopic liquid–solid wetting angle θ subtended at the three-phase contact line where the vapor, liquid and solid phases converge [2]. Henceforth, we shall delineate the distinction between *static* and *spontaneous electrowetting.* A force balance at the contact line (Fig. 2) yields Young's equation,

$$\gamma_{LV}\cos\theta = \gamma_{SV} - \gamma_{SL}\,, \tag{3}$$

where γ_{LV}, γ_{SV} and γ_{SL} are the vapor–liquid, vapor–solid and liquid–solid interfacial tensions, respectively. Substituting Eq. (3) into Eq. (1) with $\gamma = \gamma_{SL}$ gives

$$\frac{\mathrm{d}\cos\theta}{V\,\mathrm{d}V} = \frac{C}{\gamma_{LV}}\,, \tag{4}$$

which then leads to the equivalent Lippmann condition for electrowetting:

$$\cos\theta = \cos\theta_0 + \frac{\varepsilon_0\varepsilon_1 V^2}{2d\gamma_{LV}}\,, \tag{5}$$

where θ_0 is the contact angle in the absence of an electric field. The electric field has changed the vapor–liquid surface force and hence altered the static contact angle when all three surface forces balance.

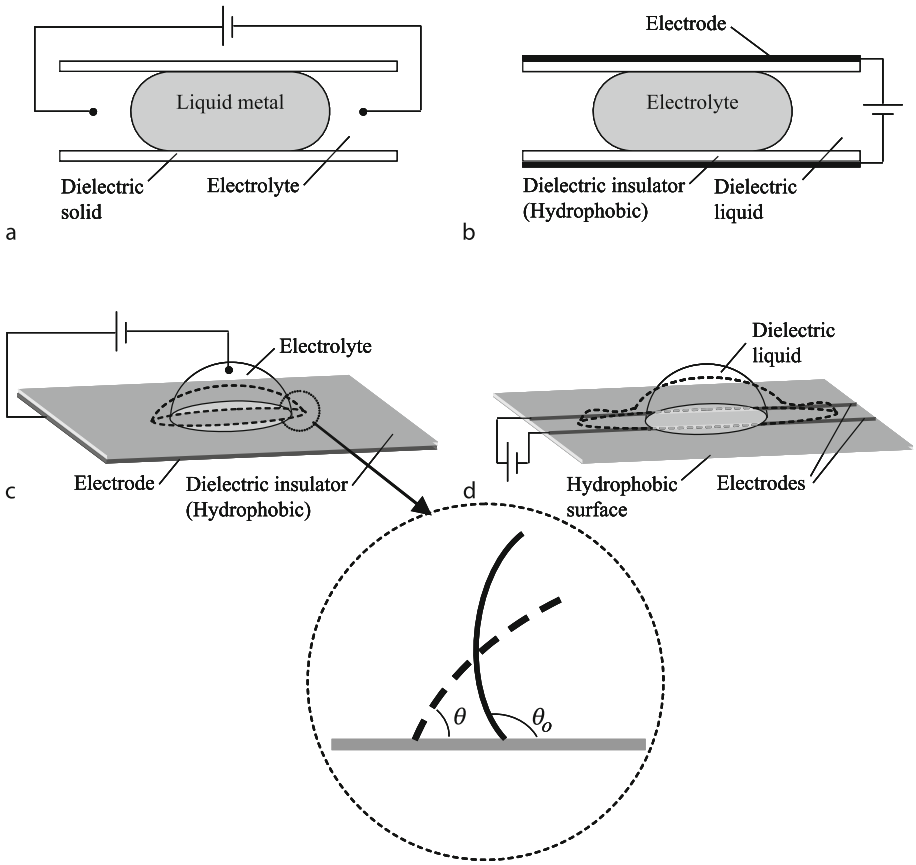

Electrowetting, Figure 1 Schematic illustration of the various electrode configurations used to demonstrate electrocapillary and electrowetting phenomena. (**a**) Electrocapillary phenomena involving a static change in the liquid metal–electrolyte contact angle. (**b**) Dielectric film coated top and bottom plate electrodes giving rise to static changes in the liquid–solid contact angle. (**c**) Dielectric film coated planar plate electrode giving rise to static changes in the liquid–solid contact angle. (**d**) Planar parallel line electrode configuration giving rise to spontaneous and dynamically advancing thin electrowetting films [2]. The inset shows an enlargement of the contact line region for case (**c**) wherein the macroscopic drop contact angle is altered from its equilibrium value θ_0 given by the Young equation to a new equilibrium value θ upon application of an electric field

The incorporation of a dielectric layer would result in a larger potential drop and a corresponding reduction in the capacitance. As most of the potential drop now occurs across the dielectric layer, the Lippmann condition in Eq. (5) can be written as

$$\cos\theta = \cos\theta_0 + \frac{\varepsilon_0 \varepsilon_d V^2}{2d\gamma_{LV}}, \tag{6}$$

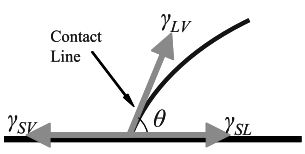

Electrowetting, Figure 2 Surface forces acting at the contact line

where ε_d is the permittivity of the dielectric layer, which is much smaller than ε_l. The above assumes the double layer capacitance, which is in series with the dielectric layer capacitance, to be negligible; this is not unreasonable given that the thickness of the double layer is typically much smaller than the dielectric layer thickness d, at least for conducting liquids. In any case, the reduction in the electric field intensity for electrowetting due to the presence of the dielectric layer requires a larger applied voltage to achieve the same electrowetting effect obtained in the absence of the dielectric layer. However, any increases in the applied voltage is restricted by a threshold voltage above which dielectric breakdown of the material occurs. Dielectric breakdown at these increased applied voltages can however be avoided by employing an AC field with a forcing frequency that is above the inverse of the RC time scale (R being the resistance of the bulk electrolyte

and C the dielectric layer capacitance) such that the potential drop across the dielectric layer is minimized.

Spontaneous electrowetting, in contrast, can arise using the parallel line electrode configuration shown in Fig. 1d, in what we shall term as *electrowetting on line electrodes* (ELE). This was first observed by Jones et al. [3], who noticed that a thin liquid film, several microns thick, is pulled out ahead of the macroscopic spreading drop when an electric potential is applied across the line electrodes, and advances much faster than the macroscopic spreading drop itself. This spontaneous and dynamically advancing film arises due to a bulk electric pressure gradient in the contact line region, which produces a negative capillary pressure that induces bulk liquid to flow into the contact line region, thus spontaneously pushing out a thin electrowetting film ahead of the macroscopic drop [2, 4].

Key Research Findings

Figure 3 shows a typical contact angle response to the applied voltage when the EWOD/EICE configuration is adopted. The observed change in the contact angle is *static* and proportional to the square of the voltage, and thus universally described by the Lippmann condition in Eq. (6) up to a limiting value in the voltage before complete wetting is achieved when deviation begins to occur. This is attributed to contact line saturation. In addition, near the saturation point, contact angle hysteresis is observed: The receding contact angle upon decreasing the voltage is observed to be smaller than the advancing contact angle at increasing voltage. It should be noted that this hysteresis effect is distinct from the usual contact angle hysteresis that occurs in drops on inclined planes, where the receding contact angle is always greater than the advancing contact angle.

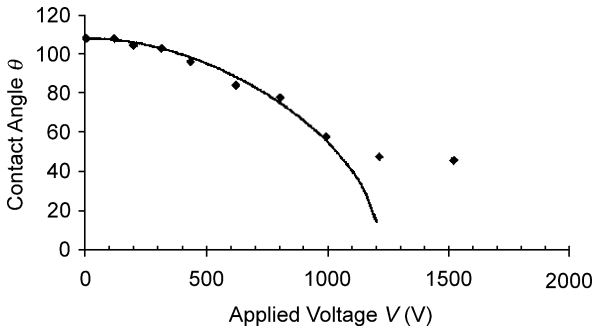

Electrowetting, Figure 3 Typical contact angle/voltage response in electrowetting-on-dielectric (EWOD) experiments. This particular set of experimental data corresponds to a 75% aqueous glycerol drop sitting above a 100 μm poly(tetrafluoroethylene) dielectric layer under an applied AC field [5]

Contact line saturation has been attributed to several factors, although these are not well understood and it may be possible that these different factors could each give rise to saturation independent of the other [6]. One possible factor is the dielectric breakdown of the atmosphere in the contact line region. When the atmosphere ionizes, the ambient phase no longer acts as an insulator wherein the charges that accumulate at the contact line exert an outwardly directed electric force which gives rise to the spreading. As a result, the leakage of charges into the ambient phase weakens this force, thus suppressing the electrowetting effect [7]. When the ambient medium is water surrounding a dielectric liquid drop, contact line saturation has been suggested to arise due to charge leakage from the aqueous phase into the insulating polymer layer at high field intensities [8]. It has also been suggested that contact angle hysteresis occurs because of the delayed release of these leaked charges from the polymer surface back into the aqueous phase when the voltage is decreased. Several theoretical descriptions have been proposed to describe the electric field induced change in the macroscopic liquid–solid contact angle in *static electrowetting*. These are based on thermodynamic, molecular kinetic, electromechanic and static approaches [2]. Vallet et al. [7] and Kang [9] considered an infinite planar wedge analysis in the three-phase contact line region, as shown in Fig. 4. As the top electrode is in contact with the drop phase, represented by the wedge, it is assumed to be at constant potential, surrounded by a perfectly insulating ambient phase whose permittivity is assumed to be equal to that of the dielectric layer of thickness d. In the absence of free charges, the electrostatic potential in the ambient phase ϕ

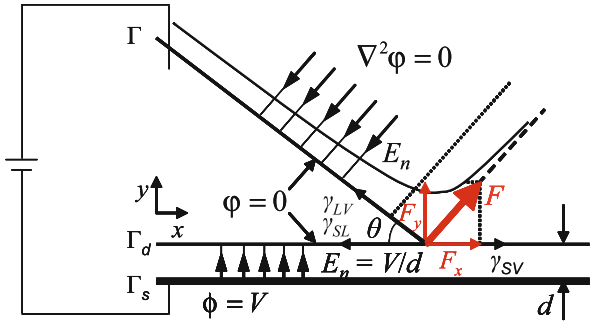

Electrowetting, Figure 4 Schematic illustration of the wedge representing the drop geometry in the contact line region in the *static electrowetting* analysis of [7] and [9]. The black arrows indicate the direction of the field and the light bold arrows indicate the resultant point force and its components at the contact line. The curve depicts the charge density or the normal field intensity along the drop interface which is singular at the tip or the three-phase contact line for all $\theta < \pi$ [2]

then obeys the Laplace equation:

$$\nabla^2\varphi = 0\,. \tag{7}$$

The boundary conditions are stipulated by the constant potential interfaces

$$\varphi = 0 \ \text{ on } \Gamma \text{ and } \Gamma_\mathrm{d} \qquad \text{and} \qquad \varphi = V \ \text{ on } \Gamma_\mathrm{s}\,, \tag{8}$$

where Γ, Γ_d and Γ_s denote the interfaces between the drop and the ambient phase, the drop and the dielectric layer and the dielectric layer and solid interfaces, respectively. Solving Eqs. (7) and (8) for small contact angles $\theta \to 0$ then yields a normal interfacial electric field that scales as

$$E_\mathrm{n}|_\Gamma \sim \frac{1}{|r|^{\frac{1}{2}}}\,, \tag{9}$$

where r is the distance along the drop interface away from the wedge tip where the contact line is located.

We note from Eq. (9) that E_n is weakly singular for $\theta < \pi$ and diverges only in a small region with length scale of order d away from the wedge tip. Since the electric pressure scales as $p_\mathrm{e} \sim E_\mathrm{n}^2$, the pressure gradient that arises as a result is localized in this small confined region at the contact line and cannot give rise to any bulk flow below the advancing contact angle. Yeo and Chang [2] also show that the solution of the biharmonic equation for the hydrodynamics within the wedge gives rise to an expression for the hydrodynamic pressure near the wedge tip as $r \to 0$ that is incompatible with the interfacial normal stress jump condition involving a singular electric stress given by Eq. (9), again suggesting the absence of any bulk flow in the contact line region. Moreover, the confined region in which the electric pressure gradient is significant is too small to be resolved in the continuum limit. As such, it is necessary to average out the electric stress, which results in a point electric force at the contact line [9]:

$$F = \frac{\varepsilon_0\varepsilon_\mathrm{d}}{2}\int_\Gamma E_\mathrm{n}^2\,\mathrm{d}r = \frac{\varepsilon_0\varepsilon_\mathrm{d}V^2}{2d}\,\mathrm{cosec}\,\theta\,. \tag{10}$$

Decomposing Eq. (10) into its horizontal and vertical components yields

$$F_x = \frac{\varepsilon_0\varepsilon_\mathrm{d}V^2}{2d}\,, \quad \text{and}\,, \quad F_y = \frac{\varepsilon_0\varepsilon_\mathrm{d}V^2}{2d}\cot\theta\,, \tag{11}$$

which, upon balancing the surface forces at the contact line, leads to the recovery of the Lippmann condition in Eq. (6). The electric pressure correction in Eq. (11) therefore accounts for the static change in the macroscopic contact angle. Since the point electric force balances the surface forces exactly, there is no net force and hence no bulk liquid flow into the contact line region. Thus, only a static change in the macroscopic contact angle results; no spontaneous electrowetting film is produced in the absence of any bulk fluid motion, therefore demonstrating why spontaneous electrowetting films cannot be produced when the EWOD/EICE configurations are adopted [2].

Yeo and Chang [4], on the other hand, have derived a lubrication model which couples the electrodynamic and hydrodynamic interactions in order to capture the formation and propagation of a spontaneous electrowetting film. Assuming a liquid with large dielectric constant, the electric field is largely confined to the liquid drop and film sitting on top of the line electrodes, as shown in Fig. 5. At the interface Γ the electric field is therefore predominantly tangential, and any normal field leakage into the ambient phase can be neglected:

$$E_\mathrm{n}|_\Gamma = -\left.\frac{\partial\varphi}{\partial z}\right|_\Gamma = 0\,. \tag{12}$$

At the line electrodes, constant potential conditions apply:

$$\varphi|_{\Gamma_\mathrm{s}} = \pm\frac{V}{2} \quad \text{at} \quad y = \mp\frac{R_\mathrm{e}}{2}\,. \tag{13}$$

In the above, x, y and z are the streamwise, transverse and vertical coordinates, respectively, and, R_e is the electrode separation.

The solution of the Laplace equation in Eq. (7) describing the potential in the liquid phase subject to the boundary conditions given by Eqs. (12) and (13) then yields the following tangential interfacial electric field near the wedge

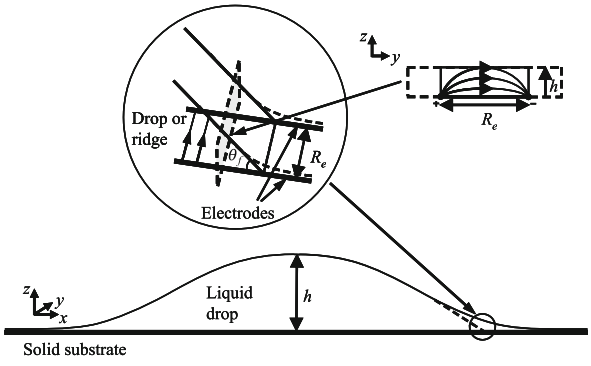

Electrowetting, Figure 5 Schematic depiction of the drop and film geometry for *spontaneous electrowetting* on parallel line electrodes. The inset shows a magnification of the contact line region in which the drop or the capillary ridge of the electrowetting film resembles a wedge-like geometry. A cross-section of this wedge and the transverse field lines arising due to the line electrodes, which resemble two point charges in this plane, is also shown [4]

tip as $h/R_e \to 0$, h being the film thickness:

$$E_t|_\Gamma = \frac{4V}{\pi R_e}\left(1 - \frac{8h^2}{R_e^2}\right) . \tag{14}$$

Given that $p_e \sim E_t^2$ and $h \sim (x_f - x)\tan\theta_f$, where x_f and θ_f are the position and contact angle of the advancing film front, the hydrodynamic pressure in the lubrication limit then reads

$$p = \gamma\frac{\partial^2 h}{\partial x^2} - \frac{8\varepsilon_0\varepsilon_1 V^2}{\pi^2 R_e^2}\left[1 - \frac{16\tan^2\theta_f}{R_e^2}(x_f - x)^2\right] , \tag{15}$$

from which we note that the hydrodynamics is enslaved to the electric field via the film thickness.

We therefore observe from Eq. (14) that the tangential field is maximum at the three-phase contact line where $h = 0$, and decays linearly along the interface away from the contact line at $x = x_f$. Unlike the *static electrowetting* case above, however, the field is non-singular in the contact line region and thus a macroscopic electric pressure gradient arises from the linearly decaying interfacial electric stress. It is this macroscopic electric pressure gradient that is responsible for a negative capillary pressure that forces liquid from the bulk into the contact line region, thus pushing out a thin spontaneous electrowetting film ahead of the macroscopic spreading drop. This is observed in the numerical results shown in Fig. 6a; we note the existence of a critical electric Bond number

$$B = \frac{8\varepsilon_0\varepsilon_1 V^2 L\tilde{L}}{\pi^2\gamma R_e^2 H} , \tag{16}$$

of approximately 10 for the formation of the electrowetting film. In Eq. (16), H and L are the characteristic height and length scales of the drop whereas $\tilde{H}$ and $\tilde{L}$ are those for the advancing film.

A dominant force balance between viscous and electric stresses at the contact line gives

$$\frac{\eta\tilde{U}}{\tilde{H}^2} \sim \frac{p_e}{\tilde{L}} , \tag{17}$$

where η is the viscosity, $\tilde{U} \sim \tilde{L}/T \equiv \gamma/\eta$ is the characteristic velocity of the film and T the time scale. It is possible to assume, consistent with the numerical results in Yeo and Chang [4] that the slope of the capillary ridge at the advancing front of the electrowetting film θ_f and the volume per unit width of the electrowetting film $V_f \sim \tilde{H}\tilde{L}$ are constant. From Eq. (15), the electric pressure gradient in Eq. (16) for constant θ_f then scales as

$$\frac{\partial p_e}{\partial x} \sim \frac{p_e}{\tilde{L}} \sim \frac{\gamma HB\tan^2\theta_f}{LR_e^2} , \tag{18}$$

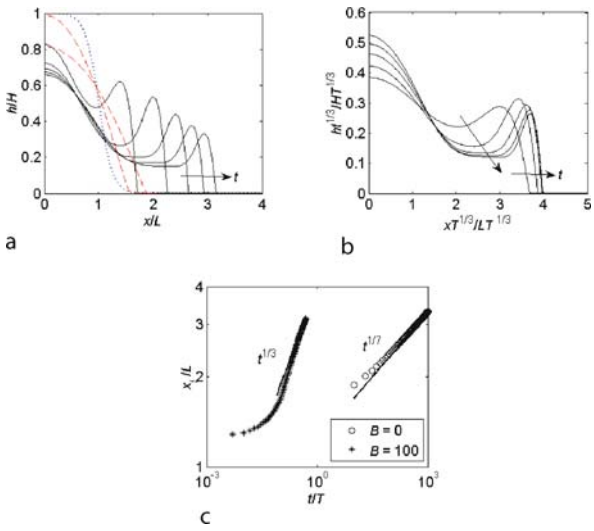

Electrowetting, Figure 6 (**a**) Transient drop and film evolution profiles for electric Bond number $B = 100$ for five equal time steps up to $t/T = 0.5$, where $T = \tilde{L}/U$ is the characteristic time scale with $U = H^3\gamma/\eta L^3$ being the characteristic system velocity. The dotted line shows the initial profile and the dashed lines indicate the spreading drop due to pure capillary motion when no electric field is applied ($B = 0$) at $t/T = 1$ and 10. (**b**) Similarity behavior of the advancing electrowetting film with the collapse of the interface profiles in time by replotting the data in (**a**) using a similarity transform. (**c**) Time dependent position of the advancing front of the drop radius or the electrowetting film x_f/L [2, 4]

which, together with Eq. (17), leads to

$$\tilde{L} \sim \left(\frac{\gamma HB\tan^2\theta_f V_0^2 T}{\eta LR_e^2}\right)^{1/3} . \tag{19}$$

Since θ_f is constant, the electric pressure gradient in Eq. (18) is also constant for a specific electrode separation R_e and hence Eq. (19) rendered dimensionless has the following similarity scaling for constant V_0:

$$x \sim t^{\frac{1}{3}} , \tag{20}$$

t being the time. Equation (20) suggests that the electrowetting film advances in a self-similar manner for electric field induced spreading. This is shown in Fig. 6b in which the film height profiles in Fig. 6a are rescaled using the similarity scaling in Eq. (20). The dynamics of the film is also shown in Fig. 6c showing that the electrowetting film advances as $t^{1/3}$, much faster than the $t^{1/7}$ behavior at which the drop spreads by pure capillary action in the absence of any electrical stresses [4]. It should be noted that the $t^{1/3}$ self-similar spreading is analogous to the self-similar gravity-driven fronts first observed by Huppert in 1982. This is because the electric pressure gradient,

given by Eq. (18) for constant θ_f acts as a constant body force term similar to gravity.

A detailed similarity analysis of the constant volume electrowetting film gives a prediction for the position of the advancing film as a function of time:

$$x_f = 0.4\left[\frac{\varepsilon_0\varepsilon_1 V^2 R_e t}{\eta}\right]^{\frac{1}{3}}. \tag{21}$$

We note therefore that the film advances independent of the dimensions and dynamics of the bulk macroscopic drop. Equation (21) can also be expressed as

$$x_f = 0.43R_e\left[\frac{t}{T_{cap}}\right]^{\frac{1}{3}}, \tag{22}$$

where

$$T_{cap} \equiv \frac{\eta L_{cap}}{\gamma} \equiv \frac{\pi^2 \eta R_e}{8\varepsilon_0\varepsilon_1 V^2}, \tag{23}$$

and

$$L_{cap} \equiv \frac{\pi^2 \gamma R_e^2}{8\varepsilon_0\varepsilon_1 V^2}, \tag{24}$$

are the electrocapillary time and length scales, respectively. Fig. 7 shows a comparison between the prediction given by Eq. (22) with data from the *spontaneous electrowetting* experiments of Ahmed et al. [11] for deionized water in which parallel line electrodes were employed, indicating close agreement without the need for any empirical fitting parameters.

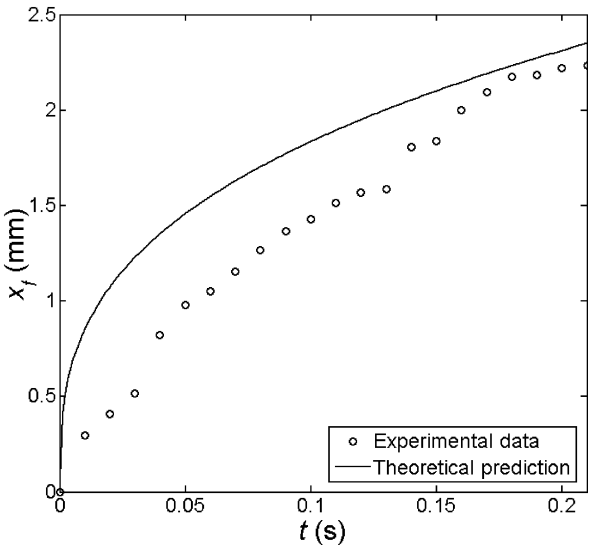

Electrowetting, Figure 7 Position of the advancing electrowetting film front x_f as a function of time t showing the close agreement between the model prediction (solid line) and the experimental data of Ahmed et al. [11] without the need for empirical fitting parameters. The experiments were carried out for deionized water ($\eta = 1$ cp , $\varepsilon_1 = 78$, $V = 200$ V and $R_e = 40$ μm); these same values were utilized for the parameters in the theoretical model [2, 4]

Examples of Application

The ability to control the wettability of a liquid, ideally without mechanically moving parts, is paramount in the handling and actuation of fluids in microfluidic devices. This has prompted a recent resurgence in electrowetting studies, which allows a rapid, reversible, and precise means for delivering and manipulating very small volumes of liquid with relatively low power consumption [10]. The success in generating fluid velocities in excess of several cm/s has also attracted significant interest in electrowetting for other applications such as electrostatic-assist coating and miniature optical focusing devices.

Cross References

- Applications Based on Electrowetting
- Digital Microfluidics
- Droplet Dispensing
- Electrocapillary
- Electrowetting and Droplets
- Interfacial Electrokinetic Flow
- Surface Tension, Capillarity and Contact Angle
- Wetting and Spreading

References

1. Quillet C, Berge B (2001) Electrowetting: A recent outbreak. Current Opinion Colloid Interface Sci 6:34–39
2. Yeo LY, Chang HC (2005) Static and spontaneous electrowetting. Modern Phys Lett B 19:549–569
3. Jones TB, Gunji M, Washizu M, Feldman MJ (2001) Dielectrophoretic liquid actuation and nanodroplet formation. J Appl Phys 89:1441–1448
4. Yeo LY, Chang HC (2006) Electrowetting films on parallel line electrodes. Phys Rev E 73:011605
5. Decamps C, De Coninck J (2000) Dynamics of spontaneous spreading under electrowetting conditions. Langmuir 16:10150–10153
6. Mugele F, Baret JC (2005) Electrowetting: From basics to applications. J Phys: Condensed Matter 17:R705–R774
7. Vallet M, Vallede M, Berge B (1999) Limiting phenomena for the spreading of water on polymer films by electrowetting. Euro Phys J B 11:583–591
8. Janocha B, Bauser H, Oehr C, Brunner H, Göpel W (2000) Competitive electrowetting of polymer surfaces by water and decane. Langmuir 16:3349–3354
9. Kang KH (2002) How electrostatic fields can change contact angle in electrowetting. Langmuir 18:10318–10322

10. Prins MWJ, Welters WJJ, Weekamp JW (2001) Fluid control in multichannel structures by electrocapillary pressure. Science 291:277–280
11. Ahmed et al. (2003) Proc. Int. Conf. Microchannels and Minichannels, ICMM2003-1110. ASME, Rochester, New York

Electrowetting, Applications

LESLIE YEO , JAMES FRIEND
Department of Mechanical Engineering,
Monash University, Clayton, VIC, Australia
leslie.yeo@eng.monash.edu.au

Synonyms

Electrowetting on dielectric (EWOD); Electrowetting on insulator coated electrodes (EICE); Electrowetting on line electrodes (ELE); Static electrowetting; Spontaneous electrowetting

Definition

Electrowetting employs an externally applied electric field to actuate or manipulate small volumes of liquid by altering its interfacial tension and hence the macroscopic contact angle or by inducing bulk liquid motion through an interfacial electric stress. Due to the low power consumption, electrowetting therefore affords an efficient, rapid, reversible, and precise means for actuating and manipulating very small volumes of liquid in microfluidic devices without the need for mechanical components.

Overview

At microscale dimensions, the surface area to volume ratio, which scales as the inverse of the characteristic length scale of the system L, becomes increasingly large, thus stipulating the dominance of surface forces over body forces. This makes it extremely difficult to move and manipulate small volumes of fluid in miniaturized fluidic devices. Several schemes that exploit Marangoni (surface tension gradient) and thermocapillary (temperature gradient) stresses to control the interfacial energy and hence drop motion have been proposed. Nevertheless, these suffer from several limitations in terms of reliability, controllability, response times and compatibility.

In contrast, the use of electrokinetics has generally been heralded as the preferred method for microfluidic manipulation due to the ease/low costs of electrode fabrication given the recent advances in micro/nano-fabrication technology, the precision and controllability afforded by electric fields, and, the reliability in the absence of mechanically moving parts. Electric field driven actuation is also rapid since the limitation is usually imposed by the hydrodynamic time scale $\mu_1 L/\gamma \sim 10^{-4}$ s, which is typically larger than the time scale for charge separation $\varepsilon_0\varepsilon_1/\kappa_1 \sim 10^{-6}$ s; μ_1, $\varepsilon_0\varepsilon_1$ and κ_1 denote the liquid viscosity, permittivity and conductivity, respectively, and γ is the interfacial tension. As such, the use of electrowetting, in which an external electric field is exploited to modify the wettability of the drop through a change in its interfacial tension or by inducing bulk motion through an interfacial stress, has become increasingly attractive as a means for microfluidic actuation and manipulation.

Yeo and Chang [1, 2] proposed that electrowetting phenomena can, in general, be classified into *static electrowetting* and *spontaneous electrowetting*, depending on the electrode configuration adopted. Static electrowetting, in which the drop sits above a planar dielectric coated plate electrode (synonymous to the configurations employed in electrowetting-on-dielectric (EWOD) or electrowetting on insulator coated electrodes (EICE); see, for example, Fig. 1a), involves the alteration of the macroscopic contact angle of the drop due to the applied electric field. It was shown in [1] through an analysis of a conducting drop that the dominant gas-phase electric field endows the drop interface with an interfacial charge and hence normal interfacial electric stress that is weakly singular towards the three-phase contact line. Nevertheless, due to the confinement of this singularity in a very small region, of the order of the dielectric coating thickness (typically microns), the interfacial stress is insufficient to result in a bulk pressure gradient in the liquid; an electric force, which can be obtained by coarse graining, simply arises at the contact line that balances the surface forces. This is shown to give rise to a modification of the macroscopic contact angle of the drop θ which obeys the Lippmann condition:

$$\cos\theta = \cos\theta_0 + \frac{\varepsilon_0\varepsilon_1 V^2}{2d\gamma_{LV}}, \tag{1}$$

where θ_0 is the equilibrium contact angle in the absence of the electric field, V the applied voltage, d the dielectric coating thickness and γ_{LV} the liquid–vapor interfacial tension.

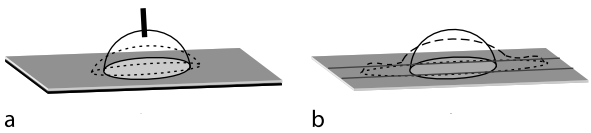

Electrowetting, Applications, Figure 1 Schematic illustration of (**a**) static electrowetting in which the applied electric field induces a macroscopic change in the contact angle, and, (**b**) spontaneous electrowetting in which a thin front-running electrowetting film is pulled out and advances ahead of the macroscopic spreading drop. The film thickness in (**b**) is not drawn to scale